Intrinsic-to-extrinsic supersolid transition and fractionally modulated states in a lattice ultracold Bose gas with long-range interaction

C.-H. Hsueh,[1] Y.-C. Tsai,[1,2] and W. C. Wu[1]

[1]*Department of Physics, National Taiwan Normal University, Taipei 11677, Taiwan*

[2]*Department of Physics, National Changhua University of Education, Changhua 50058, Taiwan*

(Received 12 June 2014; revised manuscript received 17 June 2015; published 30 July 2015)

We investigate the intrinsic-to-extrinsic supersolid (SS) transition in a lattice ultracold Bose gas with strong long-range interaction. When changing the depth of the periodic lattice potential, the transition is shown to manifest in the ground-state wave function and energy, the change of superfluid fraction f_s, and a roton instability. Near the transition in the extrinsic SS phase, due to the competition between the long-range interaction and the periodic potential, we show that there exist a variety of stable fractionally modulated states (FMSs) upon the change of the effective length of the long-range interaction. Consequence of the transition across different FMSs is discussed.

DOI: 10.1103/PhysRevA.92.013634 PACS number(s): 03.75.−b, 67.80.−s, 32.80.Ee, 34.20.Cf

I. INTRODUCTION

Supersolid (SS) is a quantum state which simultaneously possesses crystalline and superfluid (SF) properties [1–3]. Recently there is an emerging interest for the SS state in the ^{4}He system [4,5] and in the ultracold atomic system both with [6–9] and without [10–13] optical lattices. For instance, a Rydberg dressed Bose-Einstein condensate (BEC) with a controllable long-range interaction may pose a great potential to exhibit the SS state [6,14–17]. By increasing the strength of the long-range interaction, the uniform system can undergo a SF-SS transition to which a hexagonal (or triangular) lattice can form in the SS state in a two-dimensional geometry.

When the preformed intrinsic SS system is loaded into a periodic potential, upon increasing the depth of the periodic potential the system can undergo an *intrinsic-to-extrinsic* SS transition. In the intrinsic SS phase, the periodicity is governed by the effective range of the internal long-range interaction, while in the extrinsic SS phase, the periodicity is governed by the lattice constant of the external periodic potential. Motivated by the Rydberg dressed BEC, this paper intends to investigate under what circumstances the intrinsic-to-extrinsic SS transition will occur, and, how the intrinsic-to-extrinsic SS transition will manifest in experimentally observable quantities.

In the absence of the periodic potential, the role of the long-range interaction for the system is relatively well understood. However, when the periodic potential is present such that another energy scale and/or length scale mixes in, the role of the long-range interaction becomes more complex. In particular, near the intrinsic-to-extrinsic SS transition, the competition between the long-range interaction and periodic potential may cause some exotic states. It will be shown that there exists a stable "fractionally modulated state" (FMS) in which atom droplets per lattice constant is a fraction ν. More interestingly, there occurs not just one, but a variety of different fractional ν states upon the change of the effective range of the interaction. How the transition across different FMSs manifests in observable quantities, such as the superfluid fraction, will be discussed in detail.

The paper is organized as follows. In Sec. II, we introduce the basic formalism. Section II A outlines the mean-field treatment and Sec. II B outlines the Bloch band theory for the system. In Sec. III, we show that the intrinsic-to-extrinsic SS transition can be manifested by the ground-state wave function and energy (Sec. III A), the superfluid density change (Sec. III B), and a dynamical roton instability (Sec. III C). In Sec. IV, it is shown that some stable FMSs can exist in the system near the intrinsic-to-extrinsic SS transition. How the superfluid fraction changes when crossing different FMSs is also discussed. Section V studies for the intrinsic-to-extrinsic SS transition the effects of the strength and range of the interaction on the critical depth V_c of the periodic potential. Section VI is a brief summary.

II. BASIC FORMALISM

A. Mean-field treatment

As the stability of Rydberg-dressed atoms confined in an optical lattice has been confirmed [18,19], and as the dressing-induced interactions are shown to be almost the same regardless of whether in free space or in an optical lattice [19], it motivates us to consider the following mean-field treatment.

For simplicity, we focus on a one-dimensional (1D) periodic ultracold Bose system with the energy functional

$$E = \int \psi^*(x,t)\hat{h}_0\psi(x,t)dx + \frac{1}{2}\iint U(\bar{x})|\psi(x',t)|^2|\psi(x,t)|^2dx'dx. \quad (1)$$

In the first term in (1), $\hat{h}_0 = -\partial_x^2/2 + V_0\sin^2(\pi x/d)$ is the single-particle energy with d the lattice constant and V_0 the controllable depth of the periodic potential (optical lattice). Natural units $m = \hbar = 1$ are used. In the second term in (1),

$$U(\bar{x}) = \gamma\delta(\bar{x}) + \alpha\theta(r_c - |\bar{x}|), \quad (2)$$

which involves both short- and long-range two-body interactions ($\bar{x} \equiv x - x'$). To have a more systematic study on the long-range interaction, we employ a simplified step-function-like long-range interaction with α and r_c respectively the strength and effective range (or blockade radius) of the interaction. This simplified interaction gives a good approximation for the effective long-range interaction of the ultracold

Rydberg-dressed Bose gas, $U(\bar{x}) \sim \alpha/[1+(\bar{x}/r_c)^6]$ [20–23]. The corresponding Gross-Pitaevskii equation (GPE) of the system can be obtained following the differential-variational equation $i\partial_t\psi = \delta E[\psi,\psi^*]/\delta\psi^*$ together with Eq. (1).

B. Bloch band theory

It is also important to study the band structures of such a 1D periodic system, in particular, when the system is near the intrinsic-to-extrinsic SS transition and in the extrinsic SS phase. In addition, results of the lowest band is crucial in accessing the superfluid fraction of the system. Band structures of the system can be obtained by solving the Bloch waves which are the eigenstates of the nonlinear GPE. The overall time-dependent wave functions have the following form:

$$\psi(x,t) = e^{-i\mu_k t}e^{ikx}\sqrt{n_0}\varphi_k(x), \tag{3}$$

where for a given wave vector k, μ_k is the chemical potential, n_0 is the mean particle numbers per unit cell, and the Bloch wave $\varphi_k(x)$ satisfies the time-independent GPE:

$$\mu_k\varphi_k(x) = [\hat{h}_k + U_k(x)]\varphi_k(x). \tag{4}$$

Here $\hat{h}_k = -(\partial_x + ik)^2/2 + V_0\sin^2(\pi x/d)$ and

$$U_k(x) \equiv n_0\int U(\bar{x})|\varphi_k(x')|^2dx'. \tag{5}$$

As for the current system, long-range interaction is competing with the periodic potential, or more precisely the blockade radius r_c is competing with the lattice constant d, the ground state of the system may have a period longer than one lattice constant. That is, the period may be multiples of d. Under this consideration, the Bloch waves can be generally expanded as

$$\varphi_k(x) = \sum_{j=-N}^{N} a_j^k e^{i2\pi j\nu x/d}, \tag{6}$$

where based on a $(2N+1)$-mode discrete Fourier expansion, the coefficients a_j^k, assumed to be real, satisfy the normalization condition $\sum_{j=-N}^{N}(a_j^k)^2 = 1$. Typically only a few lower modes are numerically needed for a good convergent result.

The parameter ν introduced in (6) plays a key role for the current system. For a periodic system without the long-range interaction, ν can only be integer 1, corresponding to the case with the period equal to one lattice constant (d). However, for the current complex system, ν can actually be any fraction,

$$\nu \equiv \frac{n}{\ell}, \tag{7}$$

with n,ℓ the positive integers. With such a fractional ν, the period-ℓd lattice translation symmetry can be satisfied by the Bloch wave, i.e., $\varphi_k(x) = \varphi_k(x+\ell d)$. This implies that certain extrinsic SS states may correspond to a fraction ν.

III. INTRINSIC-TO-EXTRINSIC SS TRANSITION

The intrinsic-to-extrinsic supersolid (SS) transition will be shown to manifest in the ground-state wave function and energy, the superfluid fraction change, and a roton instability.

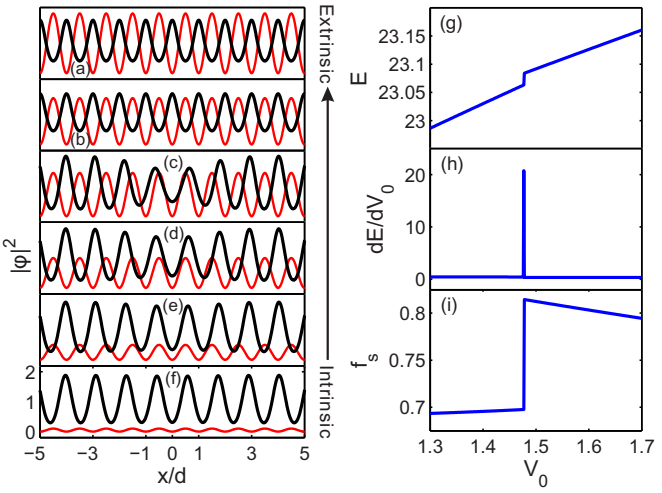

FIG. 1. (Color online) (a)–(f) Intrinsic-to-extrinsic SS transition manifested by the ground-state wave functions (black lines) of a long-range interacting lattice ultracold Bose gas. For long-range interaction, $\alpha = 30$ and $r_c = 0.75$ are fixed in all frames. Lattice potentials are schematically shown by red curves with the depth $V_0 = 2.0$, 1.55, 1.45, 1.0, 0.5, and 0.1 respectively from (a) to (f). See text for the units of energy and length. Panels (g)–(i) show the ground-state energy E, the derivative dE/dV_0, and the superfluid fraction f_s as a function of V_0 crossing the critical point at $V_c = 1.478$.

A. Ground-state wave function and energy

We have numerically solved Eq. (1) for the ground-state wave function and energy of the 1D long-range interacting lattice Bose gas using various parameters. Figures 1(a)–1(f) show the ground-state wave functions, normalized as $\int_{-d/2}^{d/2}dx|\psi(x)|^2 = 1$, with decreasing $V_0 = 2.0$, 1.55, 1.45, 1.0, 0.5, and 0.1 respectively for the lattice potential. Considering the experiment presented in Ref. [20], the total number of condensed atoms is about 10^5, which are loaded into a 100-site optical lattice, i.e., $n_0 \sim 10^3$. For the long-range interaction, we have fixed $n_0\alpha \to \alpha = 30$ and $r_c = 0.75$ in all six cases. For the short-range interaction, we simply set $\gamma = 0$ valid for the case of strong long-range interaction. Throughout this paper, all the lengths are in units of lattice constant d and all the energies are in units of $\hbar^2/md^2$. The transition is seen when the lattice potential depth V_0 is near the critical value $V_c = 1.478$ [see Fig. 1(c)]. The one near the critical regime is very profound such that two length scales appear to interfere strongly with each other.

Figures 1(g) and 1(h) show the ground-state energy E and its derivative dE/dV_0 as a function of V_0. Critical phenomena at $V_0 = V_c = 1.478$ are clearly seen in these two cases.

One might question that the extrinsic supersolid states shown in Figs. 1(a) and 1(b) may not be interpreted as the supersolids as they do not break the underlying translational symmetry. However, in our opinion, the states shown in Figs. 1(a) and 1(b) can still be viewed as a supersolid in a deep optical lattice. The point is to see how the strong lattice potential depth V_0 affects the already formed (intrinsic) supersolids shown in Figs. 1(d)–1(f). When $V_0 > V_c$, intrinsic "supersolid" is reformed (phase transitioned) to an "extrinsic supersolid" state which complies with the underlying

translational symmetry [the cases of Figs. 1(a) and 1(b)]. This is exactly the idea behind the term "intrinsic-to-extrinsic supersolid transition" introduced. Moreover, as one will see in Sec. IV, some extrinsic supersolid states, classified as the fractionally modulated states, do break the underlying translational symmetry.

B. Superfluid fraction

Superfluid fraction $f_s = \rho_s/\rho$ (ρ_s is superfluid density and ρ is total density) is a decisive measure for a given quantum system with a SF nature. In a perfect SF system, $f_s \to 1$, whereas f_s reduces from 1 when spatial modulation or dynamical fluctuation occurs, which suppresses the long-range phase coherence of SF. In the absence of lattice potential ($V_0 = 0$), Leggett showed in 1970 that one can study f_s by loading the system into a cylindrical geometry and then measure the nonclassical rotational inertial fraction (NCRIF) [3,24]. In the rest frame, the energy of the rotating system is

$$E(\omega) = E(0) + \tfrac{1}{2} I_{\rm cl}\omega^2 - \tfrac{1}{2} f_s I_{\rm cl}\omega^2, \tag{8}$$

where ω is the angular velocity and $I_{\rm cl} = mR^2$ is the classical rotational inertia with m the mass of the identical atoms loaded in a cylindrical annulus with radius R [3,24]. As the last term corresponds to the "nonrotating" superfluid part, consequently superfluid fraction f_s is proportional to NCRIF:

$$f_s = 1 - \lim_{\omega\to 0} \frac{1}{I_{\rm cl}} \frac{\partial^2 E(\omega)}{\partial \omega^2}. \tag{9}$$

Recent observation of a possible SS phase in solid ^{4}He was in fact based on measuring the NCRIF [4], although a more recent experiment has filed an opposition on the original interpretation of the previous results [5].

In a lattice system, it had been shown by Pitaveskii that the superfluid fraction is equal to the ratio of bare to effective band mass of the system, $f_s = m/m^*$ [25]. That is, reduction of f_s is compensated by the increase of the effective mass m^*. For a 1D periodic ultracold Bose system, one thus has

$$f_s = \frac{m}{m^*} = \lim_{k\to 0} \frac{m}{\hbar^2} \frac{\partial^2 E_1(k)}{\partial k^2}, \tag{10}$$

where $E_1(k)$ denotes the lowest Bloch band [26–29]. Recently an effective band mass of a periodic ultracold Bose system has been successfully measured by the Toronto group [30].

Using the Bloch band theory outlined in Sec. II B, we have solved the lowest Bloch band E_1 of the corresponding system. Based on (10), we then obtain the results of the superfluid fraction f_s as a function of V_0 shown in Fig. 1(i). A critical phenomenon at $V_0 = V_c$ is seen as a sudden jump of f_s. More results of f_s are given in Sec. IV.

C. Roton instability

It is also useful to study the elementary excitation of the corresponding ground states. The key is to investigate whether the results remain energetically minimum against perturbations that break the periodicity and especially how the intrinsic-to-extrinsic SS transition manifests. The perturbations can be decomposed into different plane-wave modes labeled by q:

$$\delta\varphi_{k,q}(x,t) = u_{k,q} e^{iqx} e^{-i\omega_{k,q}t} + v^*_{k,q} e^{-iqx} e^{i\omega^*_{k,q}t}. \tag{11}$$

The corresponding Bogoliubov–de Gennes (BdG) equations are then given by

$$\hat{\sigma}_3 M_{k,q} \begin{pmatrix} u_{k,q} \\ v_{k,q} \end{pmatrix} = \omega_{k,q} \begin{pmatrix} u_{k,q} \\ v_{k,q} \end{pmatrix}, \tag{12}$$

where

$$\hat{\sigma}_3 = \begin{pmatrix} 1 & 0 \\ 0 & -1 \end{pmatrix}$$

and

$$M_{k,q} = \begin{bmatrix} \mathcal{L}_{q+k}(x) + U_k(x) & 0 \\ 0 & \mathcal{L}_{q-k}(x) + U_k(x) \end{bmatrix} + \begin{bmatrix} C_{k,q}(x)\varphi_k(x) & X_{k,q}(x)\varphi_k(x) \\ C_{k,q}(x)\varphi^*_k(x) & X_{k,q}(x)\varphi^*_k(x) \end{bmatrix} \tag{13}$$

is an $(8N+2)\times(8N+2)$ matrix with $\mathcal{L}_{q\pm k}(x) \equiv (q \pm k)^2/2 + V_0 \sin^2(\pi x/d) - \mu_k$, $C_{k,q}(x) \equiv n_0 \int U(\bar{x})\varphi^*_k(x') e^{iq\bar{x}} dx'$, and $X_{k,q}(x) \equiv n_0 \int U(\bar{x})\varphi_k(x') e^{iq\bar{x}} dx'$.

Based on the above BdG equations, we have calculated the dispersions $\omega_{k,q}$ of the elementary excitations for an ultracold 1D nonlinear SF or SS system in the $k \to 0$ limit. As a reference, in Fig. 2(a) we first show the calculated results for the case without the periodic potential ($V_0 = 0$). The blockade radius is fixed at $r_c = 0.75$. By increasing the interaction strength α, one sees the well-known roton instability when $\alpha > \alpha_c \simeq 24.95$. It signals that the ground state is dynamically unstable against homogeneity and the system tends to modulate and form the intrinsic SS phase.

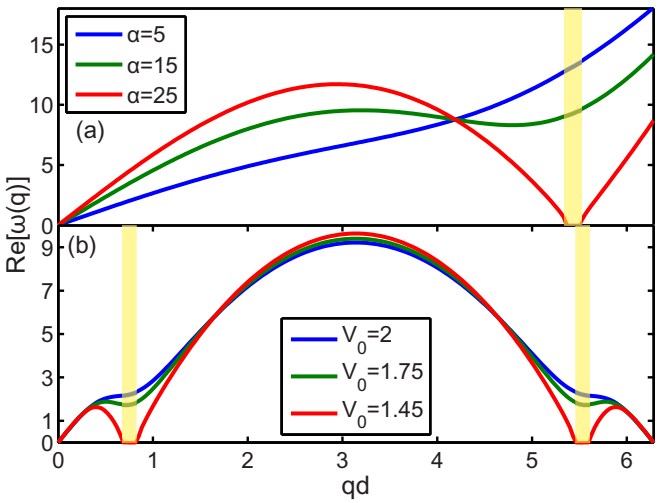

FIG. 2. (Color online) (a) Roton instability occurred in the elementary excitations of a 1D homogeneous ultracold Bose gas ($V_0 = 0$) when the long-range interaction strength α is above a critical value $\alpha_c \simeq 24.95$. Blockade radius is fixed at $r_c = 0.75$. (b) Roton instability occurred in the elementary excitations of a lattice system when the lattice potential depth V_0 is below a critical value $V_c \simeq 1.478$. The interaction strength and range are fixed at $\alpha = 30$ ($>\alpha_c$) and $r_c = 0.75$. In both frames, yellow zone corresponds to $\mathrm{Im}(\omega) \neq 0$ for the red curve.

On the contrary, Fig. 2(b) shows another roton instability for the lattice system ($V_0 \neq 0$). For the long-range interaction, $\alpha = 30$ (above α_c) and $r_c = 0.75$ are fixed. For the periodic potential, starting from a higher V_0 such that the extrinsic SS preforms and by reducing V_0 to below a critical value $V_c = 1.478$, one sees a roton instability that signals the extrinsic SS phase governed by the periodic potential becoming unstable. Consequently the system undergoes a transition to the intrinsic SS phase. How the critical depth V_c depends on α and r_c will be discussed in Sec. V.

It is worth noting that the roton instability shown in Fig. 2(a) is due purely to the interaction effect and when the instability occurs the excitation spectrum touches $\omega = 0$ at a given wave vector associated with the blockade radius. On the other hand, the roton instability shown in Fig. 2(b) is due to a mixed effect of the interaction and the lattice. The spectra shown in Fig. 2(b) are periodic with the reciprocal-lattice vector $\bar{q} = 2\pi/d$ and when the instability occurs, the spectrum touches $\omega = 0$ at two wave vectors q_1 and q_2 that satisfy $q_1 + q_2 = \bar{q}$.

In both cases of roton instabilities, after the instability occurs, the system undergoes a transition to the true ground states. How the elementary excitations behave in these true ground states [14,31] and especially how the roton restabilizes in these true ground states will be studied in details in a forthcoming paper [32].

IV. FRACTIONALLY MODULATED STATES

In the extrinsic SS phase with band character, one can investigate properties of the system based on the Bloch band theory outlined in Sec. II B. Substitution of (6) in (5) yields

$$U_k(x) = n_0 \sum_{j,j'=-N}^{N} a_j^k a_{-j'}^{k*} \tilde{U}[2\pi(j+j')\nu] e^{i2\pi(j+j')\nu x/d}, \tag{14}$$

where

$$\tilde{U}(p) = \gamma + \left(\frac{2\alpha r_c}{d}\right) \frac{\sin(pr_c/d)}{pr_c/d} \tag{15}$$

is the Fourier transform of the two-body interaction $U(\bar{x})$ given in (2). As shown explicitly in (14) and (15), $U_k(x)$ and hence the k-dependent Bloch wave $\varphi_k(x)$ [see Eq. (4)] will depend strongly on the values of r_c and α. In addition, as mentioned earlier, the fraction ν also plays an important role in the current complex system. As a matter of fact, there could exit a rich phase diagram for the ground states in the extrinsic SS phase. In particular, near the intrinsic-to-extrinsic transition, it will be shown that there exist a variety of fractionally (ν) modulated SS states for the system.

In the basis of Bloch band theory, ground states can be obtained by taking the $k \to 0$ limit in the Bloch wave of the lowest band, i.e., $\varphi_{k\to 0}(x)$. Here one can estimate for a given α what set of (ν, r_c) a particular SS ground state will correspond to. Let us first assume that chemical potential μ_k is approximately proportional to U_k by ignoring the effect of the single-particle term $\hat{h}_k$ in Eq. (4). For a given k, the leading-order term in the expansion of U_k in (14) is $\tilde{U}[2\pi(j+j')\nu]_{(j,j')=(0,0)} = \tilde{U}(0) = \gamma + 2\alpha r_c/d$ which plays as a datum point for the chemical potential. The next-order term $\tilde{U}[2\pi(j+j')\nu]_{(j,j')=(\pm1,0)\text{or}(0,\pm1)} = \tilde{U}(2\pi\nu) = \gamma + \alpha/(\nu\pi)\sin(2\pi\nu r_c/d)$ is an oscillatory

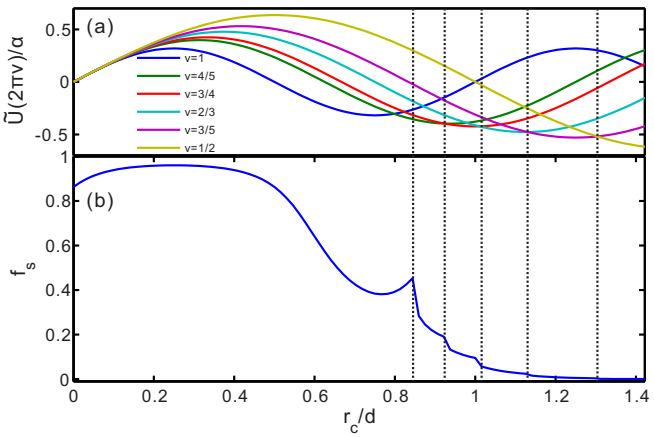

FIG. 3. (Color online) (a) $\tilde{U}(2\pi\nu)/\alpha$ plotted as a function of r_c/d for $\nu = 1$ (blue), 4/5 (green), 3/4 (red), 2/3 (cyan), 3/5 (magenta), and 1/2 (gold) respectively. For a given r_c, the ground state can be estimated corresponding to a particular ν which makes $\tilde{U}(2\pi\nu)/\alpha$ minimum (see text). (b) The calculated superfluid fraction f_s as a function of r_c/d, with fixed $\alpha = 30$ and $V_0 = 11$, showing transitions across various fractionally modulated states.

function of $\nu r_c/d$ and scales with α/ν. An estimation to determine the ground states is thus the following. For a given value of r_c/d, whatever ν makes $\tilde{U}(2\pi\nu)$ minimum will determine the ground state. In addition, when a particular fraction $\nu = n/\ell$ makes $\tilde{U}(2\pi\nu)$ minimum, the ground state will have a period of ℓd and over this period there will be n atom droplets (see Fig. 4).

Figure 3(a) plots $\tilde{U}(2\pi\nu)/\alpha$ as a function of r_c/d for six representative ν's: $\nu = 1, 4/5, 3/4, 2/3, 3/5$, and $1/2$ respectively. Again we set $\gamma = 0$ for simplicity. With increasing the value of r_c/d, the ν which makes $\tilde{U}(2\pi\nu)/\alpha$ minimum are from the left to the right $\nu = 1, 4/5, 3/4, 2/3, 3/5$, and $1/2$ accordingly.

Of course the exact ground states, subject to the examination of stability, should be obtained by solving the full differential equation (4) taking into account the single-particle term as

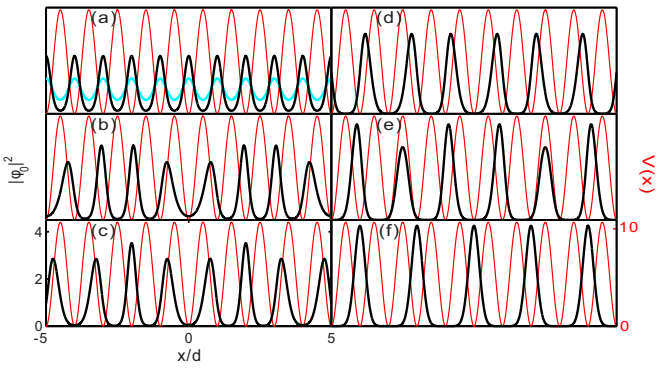

FIG. 4. (Color online) Fractionally modulated states revealed by the $k = 0$ Bloch wave density distribution $|\varphi_{k=0}|^2$ of the lowest band. The blockade radius $r_c/d = 48/64$ (a), 57/64 (b), 62/64 (c), 68/64 (d), 78/64 (e), and 87/64 (f) (black curves), which correspond respectively to $\nu = 1, 4/5, 3/4, 2/3, 3/5$, and $1/2$ states (see Fig. 3). For comparison, the cyan curve in (a) is for $r_c/d = 30/64$, which corresponds to $\nu = 1$ as well, but has relatively minor modulation. Thin red curves represent schematically the fixed lattice potential. $V_0 = 11$ and $\alpha = 30$ are fixed in all frames.

well. In principle, all fraction ν should be considered as the possible candidates for solutions. A thorough numerical study and examination has revealed that for the system with fixed $\alpha = 30$ and $V_0 = 11$, some categories of ν will not result in energetically favorable or stable ground states. It includes those with $1 > \nu > 4/5$ and $\nu > 1$. For instance, the $\nu = 5/6$ state with five droplets distributing over six lattice constants is not permitted due to energy being too high, while the $\nu = 2$ state with two droplets per lattice constant is not stable, which is easily reduced to the $\nu = 1$ state with one droplet per lattice constant. It is also not difficult to perceive that the states with $\nu = n/\ell$ with large n and ℓ are typically not energetically favorable nor stable.

We have solved the lowest Bloch band for each possible ν state with fixed $\alpha = 30$ and $V_0 = 11$ and have calculated the corresponding superfluid fraction f_s based on the effective mass scheme [Eq. (10)]. Figure 3(b) shows the calculated superfluid fraction f_s as a function of r_c/d. As mentioned earlier, for the current system only those states with $\nu = 1$ and $\nu = n/\ell < 4/5$ (for n and ℓ not being too large) are available. In view of Fig. 3(b), phase transitions across different fraction ν states are manifested either by a jump or by a drop of f_s. These jumps or drops arise due to the "discontinuity" or "forbiddance" of some fractional ν states. The state with $\nu < 1/2$ such as $\nu = 1/3$ is actually permitted and corresponds to a modulation of one droplet per three lattice constants. However, the superfluid fraction f_s is sufficiently reduced and the SS state is no longer justified (the system is perhaps in the solid phase).

To view the possible fractionally modulated states in an evident way, Figs. 4(a)–4(f) plot the ground-state density distribution, $\rho(x) \equiv |\varphi_{k=0}(x)|^2$. To make a contact with the results in Fig. 3, it has been chosen that $r_c/d = 48/64, 57/64, 62/64, 68/64, 78/64$, and $87/64$, respectively in panels (a)–(f). $V_0 = 11$ and $\alpha = 30$ are fixed in all frames. These correspond to $\nu = 1$, $4/5$, $3/4$, $2/3$, $3/5$, and $1/2$ modulated SS states respectively. As shown explicitly, the $\nu = 2/3$ state [panel (d)] has two atom droplets every three lattice constants ($3d$), while the $\nu = 1/2$ state [panel (f)] has one atom droplet every two lattice constants ($2d$). In panel (a), we also show $\rho(x)$ for $r_c/d = 30/64$ (cyan curve). This case, also corresponding to the $\nu = 1$ state, has relatively minor modulation compared to that of the $r_c/d = 48/64$ case.

V. CRITICAL DEPTH V_c

For the intrinsic-to-extrinsic SS transition, we here discuss the effects of the interaction strength α and the blockade radius r_c on the critical depth V_c of the lattice potential. In our studies, V_c is defined as the critical depth at which the $\nu \neq 1$ state undergoes a transition to the $\nu = 1$ state or vice versa.

Figure 5(a) shows the results of V_c as a function of α. For a given r_c, the curve stars from the corresponding critical strength α_c for the SF to the intrinsic SS transition (the dot). As seen, α_c is smaller for the case with larger r_c. It is perceived that larger r_c means more effectiveness for the long-range interaction and the roles of α and r_c are counterparts in the absence of the external potential. As a matter of fact, a somewhat universal dimensionless number, $\alpha_c r_c^3 \approx 10$, exists among the three curves shown in Fig. 5(a). Once $\alpha > \alpha_c$, V_c rises monotonically as α increases as they compete with each other. In the present complex system, however, in addition to competition α also plays the role for stabilizing the extrinsic SS state. As a consequence, the V_c curve will drop for larger α and eventually decrease to zero when α is larger than a certain value. In the latter case, it means that the extrinsic SS state is robust so long as $V_0 > 0$.

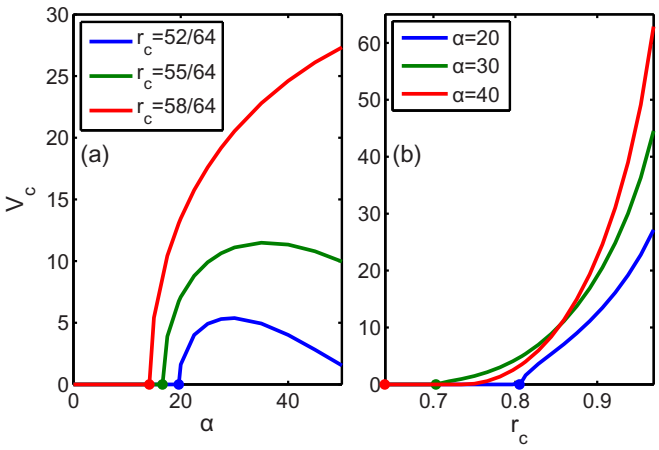

FIG. 5. (Color online) (a) Critical depth V_c of the lattice potential as a function of α for three different r_c. The dots correspond to critical strength α_c for the SF-to-intrinsic SS transition when $V_0 = 0$. (b) Critical depth V_c as a function of r_c for three different α. The dots correspond to critical length r_c for the SF-to-intrinsic SS transition when $V_0 = 0$.

Figure 5(b) shows the effect of the blockade radius r_c on V_c. As seen for a given α, the curve starts from a critical r_c for V_c to be finite (the dot). In general, a smaller α case corresponds to a larger critical r_c which again states the counterpart roles of α and r_c. Once r_c is above the critical value, V_c increases with the increasing r_c. It was pointed out that a relatively smaller-ν fractionally modulated state can form for relatively larger r_c (see Fig. 3). And generally it requires a stronger V_c to reform the $\nu = 1$ extrinsic SS state from a relatively smaller $\nu < 1$ state.

VI. SUMMARY

In summary, the intrinsic-to-extrinsic supersolid (SS) transition is investigated in a lattice ultracold Bose gas with strong long-range interaction. It is demonstrated that the transition is manifested in the ground-state wave function or energy, the change of superfluid fraction f_s, and a roton instability. Due to the competition between the long-range interaction and the periodic potential, we show that there exist a variety of stable fractionally modulated states near the intrinsic-to-extrinsic SS transition in the extrinsic SS phase. The transition across different fractionally modulated states is evidenced by either a superfluid fraction jump or a drop.

ACKNOWLEDGMENTS

We are grateful to S. Yip (Academia Sinica) for very useful comments. The support from the Ministry of Science and Technology, Taiwan (under Grant No. NSC 102-2112-M-003-015-MY3) and the National Center of Theoretical Sciences of Taiwan are acknowledged.

[1] A. F. Andreev and I. M. Lifshitz, Sov. Phys. JETP **29**, 1107 (1969).
[2] G. V. Chester, Phys. Rev. A **2**, 256 (1970).
[3] A. J. Leggett, Phys. Rev. Lett. **25**, 1543 (1970).
[4] E. Kim and M. H. W. Chan, Nature (London) **427**, 225 (2004); Science **305**, 1921 (2004).
[5] D. Y. Kim and M. H. W. Chan, Phys. Rev. Lett. **109**, 155301 (2012).
[6] B. Capogrosso-Sansone, C. Trefzger, M. Lewenstein, P. Zoller, and G. Pupillo, Phys. Rev. Lett. **104**, 125301 (2010).
[7] L. Pollet, J. D. Picon, H. P. Büchler, and M. Troyer, Phys. Rev. Lett. **104**, 125302 (2010).
[8] M. Iskin, Phys. Rev. A **83**, 051606 (2011).
[9] A. Bühler and H. P. Büchler, Phys. Rev. A **84**, 023607 (2011).
[10] N. Henkel, R. Nath, and T. Pohl, Phys. Rev. Lett. **104**, 195302 (2010).
[11] G. Pupillo, A. Micheli, M. Boninsegni, I. Lesanovsky, and P. Zoller, Phys. Rev. Lett. **104**, 223002 (2010).
[12] F. Cinti, P. Jain, M. Boninsegni, A. Micheli, P. Zoller, and G. Pupillo, Phys. Rev. Lett. **105**, 135301 (2010).
[13] C.-H. Hsueh, Y.-C. Tsai, K.-S. Wu, M.-S. Chang, and W. C. Wu, Phys. Rev. A **88**, 043646 (2013).
[14] T. Macrì, F. Maucher, F. Cinti, and T. Pohl, Phys. Rev. A **87**, 061602(R) (2013).
[15] K. Góral, L. Santos, and M. Lewenstein, Phys. Rev. Lett. **88**, 170406 (2002).
[16] N. Henkel, F. Cinti, P. Jain, G. Pupillo, and T. Pohl, Phys. Rev. Lett. **108**, 265301 (2012).
[17] C.-H. Hsueh, T.-C. Lin, T.-L. Horng, and W. C. Wu, Phys. Rev. A **86**, 013619 (2012).
[18] W. Li, C. Ates, and I. Lesanovsky, Phys. Rev. Lett. **110**, 213005 (2013).
[19] T. Macrì and T. Pohl, Phys. Rev. A **89**, 011402 (2014).
[20] M. Viteau, M. G. Bason, J. Radogostowicz, N. Malossi, D. Ciampini, O. Morsch, and E. Arimondo, Phys. Rev. Lett. **107**, 060402 (2011).
[21] M. Mattioli, M. Dalmonte, W. Lechner, and G. Pupillo, Phys. Rev. Lett. **111**, 165302 (2013).
[22] J. E. Johnson and S. L. Rolston, Phys. Rev. A **82**, 033412 (2010).
[23] J. Honer, H. Weimer, T. Pfau, and H. P. Büchler, Phys. Rev. Lett. **105**, 160404 (2010).
[24] A. J. Leggett, J. Stat. Phys. **93**, 927 (1998).
[25] L. P. Pitaveskii, in *Nonlinear Waves: Classical and Quantum Aspects*, edited by F. Kh. Abdullaev and V. V. Konotop (Kluwer Academic, Amsterdam, 2004), pp. 175–192.
[26] B. Wu and Q. Niu, Phys. Rev. A **64**, 061603 (2001).
[27] B. Wu, R. B. Diener, and Q. Niu, Phys. Rev. A **65**, 025601 (2002).
[28] D. Diakonov, L. M. Jensen, C. J. Pethick, and H. Smith, Phys. Rev. A **66**, 013604 (2002).
[29] Y. Y. Lin, R.-K. Lee, Y.-M. Kao, and T.-F. Jiang, Phys. Rev. A **78**, 023629 (2008).
[30] R. Chang, S. Potnis, R. Ramos, C. Zhuang, M. Hallaji, A. Hayat, F. Duque-Gomez, J. E. Sipe, and A. M. Steinberg, Phys. Rev. Lett. **112**, 170404 (2014).
[31] S. Saccani, S. Moroni, and M. Boninsegni, Phys. Rev. Lett. **108**, 175301 (2012).
[32] C.-H. Hsueh, Y.-C. Tsai, and W. C. Wu (unpublished).